Corium Shield and Pedestal Flooding Severe Accident Analysis for Small Modular Reactor BWRX-300

Nassim Sahboun[a*], Takayuki Someya[a], Tomohiko Ikegawa[a], Home DEEPAYAN[b]
[a]Hitachi-GE Nuclear Energy,Ltd., Hitachi, Japan
[b]GE Hitachi Nuclear Energy-GE Vernova, Markham, Canada

Abstract: In the case of the small modular reactor (SMR) BWRX-300 developed by GE-Hitachi, preliminary probabilistic safety assessment (PSA) has identified several severe core damage accident scenarios, primarily Loss-of-Coolant Accidents (L◦CA) and general transient events, which could lead to the rel◦Cation of corium from the reactor pressure vessel (RPV) to the primary containment vessel (PCV) pedestal. Without any countermeasures, this could result in the erosion of the pedestal concrete due to molten corium concrete interaction (MCCI), causing severe heating and over-pressurization of the containment vessel, potentially leading to PCV damage and leaks.
To practically eliminate MCCI and ensure the integrity of the PCV under these severe accident scenarios, two countermeasures have been proposed: (a) a corium shield made of refractory material integrated onto the pedestal floor and side walls, and (b) the addition of water to the pedestal.
A severe accident analysis (SAA) was conducted to evaluate the effectiveness of the designed corium shield and pedestal water addition strategies in meeting the imposed safety limits. This article presents the modeling process carried out using the Modular Accident Analysis Code (MAAP5) [1] and the results of the SAA for the SMR BWRX-300. The SAA results indicate that the proposed countermeasures are effective in practically eliminating MCCI.

Keywords: Nuclear, Severe Accident, Small Modular Reactor

1. INTRODUCTION

As part of the evolution of the nuclear industry post Fukushima, SAA has become a necessary part of the design pr◦Cess for new NPP. As such, the emerging new generation of NPP like the SMR type has a need for SAA to help validate and/or improve its design, even in the early stage of its conception. Currently, one of the challenging points for the new generation of NPP is the safety measures concerning MCCI and the validation of their effectiveness.
In this present article, we try to answer this challenge for the SMR BWRX-300 by investigating the use of a combination of corium shield and pedestal passive water addition (severe accident water addition (SAWA) strategy) as MCCI countermeasures. These countermeasures were selected to complete the following goal: improve the current BWRX-300 design to allow to practically eliminate MCCI.
With these goals in perspective, this article is divided in the following manner.

- MAAP modeling used in the present study
- Sequence and conditions used for the present SAA
- Discussion of the results and their implication for the BWRX-300 design
- Conclusions

2. MAAP MODELING

As previously mentioned, following the events at Fukushima Daichi NPP accident, nuclear regulations went through a series of reform that highlights and make mandatory countermeasures for MCCI, for both old and new NPP. One such countermeasure is a combination of corium shield and pedestal water addition. This is the focus of SAA performed for BWRX-300 in the present article. The SA code MAAP ver5.06 [1] was used for performing the simulations.
The present section discusses in more detail the design of the corium shield and pedestal water addition that is modelled in MAAP for SAA.
After reviewing the corium shield designs used in the existing BWRs, it has been found that generally the corium shield design fall under the following two types:

1) Floor and/or wall type corium shield
2) Weir type corium shield

The floor and/or wall type corium shield corresponds to embedding the shield material on the pedestal floor and/or wall to prevent MCCI. This design also incorporates slits large enough to allow water to pass but small enough to keep debris in the pedestal area and to prevent it from falling in the water collecting funnel under the slits as shown in Figure 2.1a.

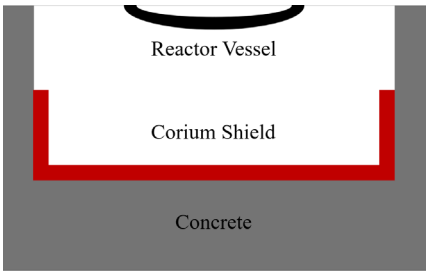

Figure 2.1a Floor type corium shield

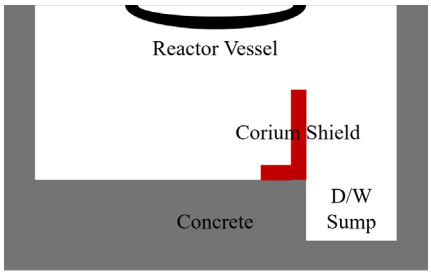

Figure 2.1b Weir type corium shield

As for the Weir type, the goal is to avoid accumulation of corium in pedestal area/zone that have any non-negligible depth, such as drain sump pit for example. This allows to avoid the formation of deep pool of debris that will be difficult to cool and prone to start MCCI.
This design also assumes that the rest of the pedestal floor area is wide enough to allow the corium to spread on a large area, therefore increasing the potential for debris cooling and preventing MCCI as shown in Figure 2.1b. As such, this type of corium shield design is more typical of larger NPP, such as ABWR plants.
For the current SMR study, the floor and/or wall type corium shield was considered to be the optimal design choice.
Potential material candidates considered for corium shield are Al_2O_3, MgO, and ZrO_2 [2]. The main proprieties of interest for the corium shield material are summarized in Table 2.1 for each of the material type. As seen in Table 2.1, ZrO_2 by far has the most desirable thermo-chemical characteristics against corium thermal attack that makes it the ideal candidate for the corium shield material.

Table 2.1 Applicability of 3 materials (Al_2O_3, MgO, and ZrO_2) to corium shield

	Zirconia (ZrO_2) [2]	Alumina (Al_2O_3)	Magnesia (MgO)
Melting temperature	2700 °C	2030 °C	2800 °C
Chemical resistance*1)	High	Middle	Low
Tolerance against erosion*2)	High	Low	Middle
Material cost*3)	High	Low	Middle

*1) Corium shield material must be chemically resistant against reduction reaction. The rank of each material is determined by comparing the standard Gibbs free energy of formation (Ellingham diagram). The chemical denudation experiment shows the same trend.
*2) The rank of each material is determined by referring to the melting temperature and the corium-corium shield interaction experiment result.
*3) The rank of each material is determined by catalogue prices of the material costs. This is not based on detailed estimation by suppliers.

Since, the chemical denudation experiment shows that the reducing reaction of MgO proceeds intensely, MgO has been excluded as material candidate The melting temperature of Al_2O_3 is low and the tolerance against erosion is low, the cost is lower compared to ZrO_2, which would be important in the design to cost approach for BWRX-300. In addition, there are design experiences for ZrO_2 and Al_2O_3 corium shield in GEH and HGNE. Therefore, ZrO_2 and Al_2O_3 are selected as the corium shield material candidates for the current BWRX-300 study.
The ratio of thermal power to the pedestal floor area estimate for various BWR plants is shown in Table 2.2. The data indicates that BWRX-300 has much higher thermal margin against MCCI compared to existing BWRs. In fact, it is anticipated that soon after the start of pedestal water addition, debris temperature will start decreasing and concrete erosion will be prevented. Thus, to practically eliminate MCCI, the corium shield thickness should be determined so that inner concrete ablation does not commence until pedestal water addition starts.

To provide some margin against phenomenological uncertainty, the minimum required corium shield thickness for both ZrO_2 and Al_2O_3 is determined by numerical solution of the 1-dimensional transient heat conduction equation with conservative assumptions. The 1-dimensional heat conduction equation without heat generation term [3] is defined as:

$$\frac{\partial T}{\partial t} = \frac{\lambda}{C_p \rho} \frac{\partial T}{\partial x^2} \quad \text{(Equation 2.1)}$$

where λ is thermal conductivity, C_p is specific heat, ρ is density.

The explicit finite difference expression for the 1-dimensional heat conduction equation for the corium shield is shown below:

$$T_k(t_{l+1}) = T_k(t_l) + \frac{\lambda}{C_p \rho} \frac{T_{k-1}(t_l) + T_{k+1}(t_l) - 2T_k(t_l)}{{\Delta x_k}^2} (t_{l+1} - t_l) \quad \text{(Equation 2.2)}$$

where $T_k(t_l)$ is corium shield nodal temperature in node k at time step t_l, Δx_k is width of node k. The number of nodal points n for this study is chosen as 20 and number of time steps m is defined by (calculation time [sec]) / (time step width (Δt) = 5 [sec]).

The discretization above satisfies the following diffusion number condition [4].

$$d = \frac{\lambda}{C_p \rho} \frac{\Delta t}{{\Delta x_k}^2} \leq \frac{1}{2} \quad \text{(Equation 2.3)}$$

The temperature dependency of the corium shield material properties (λ, C_p, ρ) is ignored and constant values are applied. To solve the equation, the following two boundary conditions and one initial condition are defined:

$$T_0(t_l) = T_s = const. \quad \text{(Equation 2.4)}$$

$$\frac{dT_n(t_l)}{dx} = 0 \ \ (Adiabatic) \quad \text{(Equation 2.5)}$$

$$T_k(t_1 = 0) = T_i = const. \quad \text{(Equation 2.6)}$$

where $k = 0$ signifies the boundary between debris and corium shield, $k = n$ signifies the boundary between corium shield and concrete, T_s is temperature of the interface between the debris and the corium shield, T_i is initial temperature of the corium shield.

As the containment vent maintains containment pressure below 225.1 kPa(a), the initial temperature T_i is set to the saturation temperature of 397 K (=124 ℃) at 225.1 kPa(a). By assuming both the debris and the corium shield wall behave as semi-infinite solids, the interface temperature T_s is approximated with the following formula [6]:

$$T_s = \frac{T_{debris,m} \sqrt{\left(k \rho C_p\right)_{debris}} + T_i \sqrt{\left(k \rho C_p\right)_{corium\ shield}}}{\sqrt{\left(k \rho C_p\right)_{debris}} + \sqrt{\left(k \rho C_p\right)_{corium\ shield}}} \quad \text{(Equation 2.7)}$$

where $T_{debris,m}$ is the melting temperature of the debris.
Applying T_i values depicted in Table 2.1, T_s is calculated for each scenario and each corium shield material type. The interface temperatures T_{s,ZrO_2} is set to 2510 K (=2237 ℃) and T_{s,Al_2O_3} is set to 1842 K (= 1569 ℃) which is used to evaluate the heat conduction equation. In the evaluation of the heat conduction equation, the interface temperature is invariant with time.
In general, the interface temperature T_s will increase gradually from the initial temperature T_i. With progression of time, corium shield temperature increases over the entire region, the semi-infinite solid approximation will not satisfy, and T_s could be higher than the value evaluated using (Equation 2.7).
However, pedestal water addition can be expected to initiate much before underestimation of T_s becomes a problem. Therefore, applying T_{s,ZrO_2} and T_{s,Al_2O_3} as constant in (Equation 2.4) is conservative.
To practically eliminate MCCI, inner concrete temperature must be below its melting temperature until pedestal water addition is initiated. Referring to the MAAP calculation result for the increase in pedestal gas

temperature, pedestal water addition timing is conservatively assumed 2.5 hours after the vessel failure. Thus, the minimum required corium shield thickness is determined so that the inner surface corium shield temperature at 2.5 hours after the vessel failure reaches the Limestone-Common Sand (LCS) concrete melting temperature (assumed to be 1312.85 ˚C [1]). The numerical calculation results for ZrO_2 and Al_2O_3 are shown in Figure 2.2a and Figure 2.2b respectively. At these conditions, the ZrO_2 corium shield thickness is 0.112 m, and the Al_2O_3 corium shield thickness is 0.131 m.
In conclusion, ZrO_2 corium shield thickness should be thicker than or equal to 0.12 m and Al_2O_3 corium shield thickness should be thicker or equal to 0.14 m.

Table 2.2 Ratio of thermal power to pedestal floor area in various BWR plants

	BWR-5		ABWR	BWRX-300
PCV type	Mark-I advanced	Mark-II	RCCV	SCCV
Thermal power [MWt]	2436	3293	3926	870
Inner diameter in pedestal [m](*)	5.5	6.2	10.6	6.64
Pedestal floor area [m^2](*)	23.8	30.2	88.2	34.6
Thermal power / Floor area [MWt/m^2]	102.3	109.0	44.5	25.1

(*) Corium shield structure is ignored.

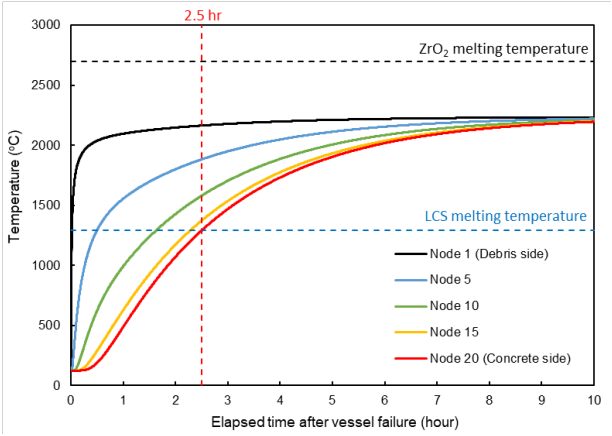

Figure 2.2a Numerical calculation result of 0.112 m thickness ZrO_2 corium shield

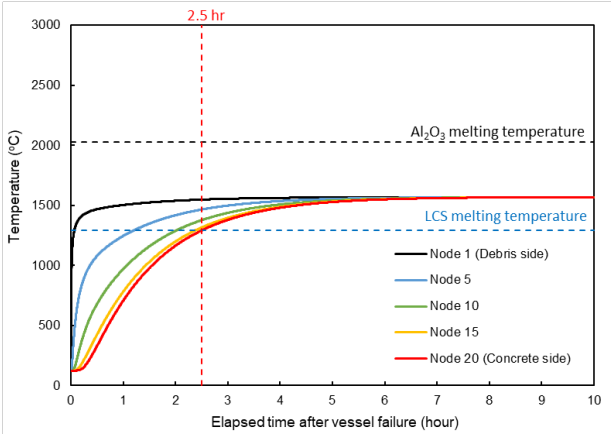

Figure 2.2b Numerical calculation result of 0.131 m thickness Al_2O_3 corium shield

For the pedestal water addition strategy, it is proposed that water addition to the pedestal be initiated after the vessel failure. This strategy is used in order to eliminate the possibility of an explosive interaction mode between the core debris melt and water.

3. ANALYSIS SEQUENCES AND CONDITIONS

From the preliminary Level 1 and Level 2 PSA, four accident sequences were selected for MAAP SAA. As a preliminary step to the work presented in this article, runs for each of the selected sequences to determine the most severe MCCI were performed. The preliminary simulations were performed without MCCI countermeasures. This preliminary step found that the large loss-of-coolant accident (LL◦CA) is the most severe sequence in relation to MCCI. Therefore, LL◦CA was chosen as the sequence to verify the effectiveness of corium shield and pedestal water addition.

Table 3.1 Analysis conditions summary [6]

Item	Value
Thermal power [MWt]	870
Heat loss from RCS [MWt]	0.165
Reactor pressure [MPa(a)]	7.17
Core flow rate [kg/s]	1764
Feed water flow rate [kg/s]	501.5
Feed water enthalpy [J/kg]	1.047×10^6
CRD flow rate [m^3/h]	4.5
CRD flow enthalpy [J/kg]	9.522×10^4
Normal water level [m]	21.48
Two-phase flow quality for coolant exiting the core [-]	0.2859

4. RESULTS AND DISCUSSION

Based on the sequence assumption introduced in section 3, minimum required corium shield thickness to prevent MCCI and containment overtemperature is surveyed for both ZrO_2 and Al_2O_3 corium shield in MAAP. The results show that inner concrete temperature and containment boundary heat sink temperature do not reach the concrete melting temperature (assumed to be 1312.85 ˚C [1]). Additionally, it has been found that MCCI does not occurred in any of the MAAP runs.

Sensitivity analysis on the corium shield thickness, for thickness smaller than the thickness predicted by hand calculation (see section 2) was also performed. It was found that the minimum required thickness to avoid MCCI predicted by MAAP is much smaller than the numerical calculation result in section 2.

It can be concluded that there is sufficiently large safety margin in the numerical evaluation of the minimum corium shield thickness for both ZrO_2 and Al_2O_3 materials.

Table 4.1 Ratio of thermal power to pedestal floor area in various BWR plants

	ZrO_2 Corium Shield				**Al_2O_3 Corium Shield**			
Base Cases	*MCCI Prevented*	Floor Erosion Depth: 0 m	*Cont. Overtemp. Avoided*	Floor Concrete Surface Temperature: ~500 ˚C	*MCCI Prevented*	Floor Erosion Depth: 0 m	*Cont. Overtemp. Avoided*	Floor Concrete Surface Temperature: ~750 ˚C
		Side Wall Erosion Depth:0 m		Side Wall Concrete Surface Temperature: ~500 ˚C		Side Wall Erosion Depth:0 m		Side Wall Concrete Surface Temperature: ~750 ˚C
Corium Shield Thickness Sensitivity Analysis Cases	*MCCI Prevented*	Floor Erosion Depth: 0 m	*Cont. Overtemp. Avoided*	Floor Concrete Surface Temperature: ~1250 ˚C	*MCCI Prevented*	Floor Erosion Depth: 0 m	*Cont. Overtemp. Avoided*	Floor Concrete Surface Temperature: ~1250 ˚C
		Side Wall Erosion Depth:0 m		Side Wall Concrete Surface Temperature: ~1300 ˚C		Side Wall Erosion Depth:0 m		Side Wall Concrete Surface Temperature: ~1300 ˚C

5. CONCLUSION

In the present article, MCCI countermeasures were presented, and their effectiveness was evaluated for their application to the SMR BWRX-300. It has been found that the coupling of the two envisioned MCCI countermeasures, corium shield and pedestal flooding, was indeed effective at preventing MCCI and practically eliminating it from BWRX-300 design.

For the corium shield, the minimum required thickness has been determined by the conservative numerical calculation to consider future design change. Since Al_2O_3 corium shield function deteriorates due to the reduction reaction by Zr in debris and ZrO_2 corium shield has favourable thermo-chemical stability, ZrO_2 corium shield is selected as the representative condition in this study. The representative condition wherein MCCI can be prevented is achieved.

However, some uncertainty and sensitivity issues remain, such as sensitivity surrounding the water addition location and mass flowrate and will be the scope of future publications.

Acknowledgements

References

[1] EPRI, MAAP5.06 User's Manual

[2] NUREG/CR-6150, Vol.4, Rev.2 (PT3) "SCDAP/RELAP5/MOD 3.3 Code Manual: MATPRO -A Library of Materials Properties for Light-Water-Reactor Accident Analysis".

[3] J. A. Gopsill, Finite Difference of the 1D Explicit Heat Equation, 2019.

[4] Courant, R., Friedrichs, K. & Lewy, H., 1928. Über die partiellen Differenzengleichungen dermathematischen Physik. Mathematische Annalen, 100(1), pp. 32-74.

[5] T. Loulou, D. Delaunay,The interface temperature of two suddenly contacting bodies, one of them undergoing phase change, International Journal of Heat and Mass Transfer,Volume 40, Issue 7,1997,Pages 1713-1716

[6] GE Hitachi Nuclear Energy, IAEA, "Status Report – BWRX-300" (PDF), 30 September 2019 (Retrieved 31 December 2023).